An investigation of the thermal stabilities of two malate dehydrogenases by comparison of their three-dimensional structures

M.L. Duffield, D.J. Nicholls, T. Atkinson, and M.D. Scawen

Division of Biotechnology, PHLS Centre for Applied Microbiology and Research, Public Health Laboratory Service, Porton Down, UK

The tertiary structure of Thermus aquaticus *malate dehydrogenase (MDH) was predicted based on the known crystal structure of pig heart cytosolic MDH. Guanidinium chloride (GdmCl) unfolding experiments showed that there is only about a 4.2-kjoule/mol difference in* ΔG° *between the pig and* Thermus *MDH. However, the two enzymes varied greatly in their* $[GdmCl]_{1/2}$*, with* Thermus *MDH showing the expected increased stability (3.20 M against 0.58 M for pig MDH). The half-lives were determined for both* Thermus *MDH (34 min at 90°C) and pig MDH (1.8 min at 60°C). The* Thermus *MDH model was then examined to see what effect the substituted residues and changes may have on the enzyme, particularly in relation to its high thermal stability.*

Keywords: protein structure prediction, thermal stability, guanidinium chloride unfolding

INTRODUCTION

Understanding the factors responsible for thermal stability is of fundamental importance. One approach to this problem is the comparison of the properties, sequences, and structures of homologous proteins from mesophilic and thermophilic sources. However, the difference in stability is often only a few kjoule/mol, therefore changes producing an increase in thermal stability can be very subtle, involving only a few extra bonding interactions. These can be masked by other changes which are not involved in thermal stability. Clearly, detailed three-dimensional structures of analogous enzymes from both mesophiles and thermophiles are needed, but such structures are not yet available.

Malate dehydrogenase (L-malate:NAD oxidoreductase, EC 1.1.1.37, MDH) catalyzes the reduction of malate to oxaloacetate (and the reverse oxidative reaction) utilizing the NADH/NAD cofactor system. In mammalian cells, two isoenzymes of malate dehydrogenase are known, both of which are synthesized in the cytoplasm. One form then transfers to the mitochondria and becomes the mitochondrial malate dehydrogenase.[1] The other, cytosolic form was among the first oligomeric enzymes to have its three-dimensional coordinates determined,[2,3] although at the time the full amino acid sequence of the protein was not known.

More recently, however, the refined molecular structure of the cytosolic malate dehydrogenase (cMDH) from pig heart has been determined to a 0.25-nm resolution.[4] This enzyme is a dimer made up of two subunits, each of 333 amino acid residues; it has two binding sites for NADH, 471 solvent molecules, and two large noncovalently bonded molecules that are assumed to be sulphate ions. The two subunits, though identical in amino acid sequence, are structurally nonequivalent in the crystalline enzyme,[5,6] possibly due to effects caused by molecular packing within the crystal lattice.[4]

The crystal structures of both the porcine heart mitochondrial (mMDH)[7] and *Escherichia coli* (eMDH)[8] malate dehydrogenases have also been determined. They are both dimeric, with subunits of 314 and 312 residues, respectively. The subunit interface of cMDH is made up predominantly of interactions between the helices[4] αB, αC, α2G, and α3G according to the nomenclature of Hill et al.[2] Similar interactions are seen between the same helices in both mMDH[7] and eMDH,[8] although in eMDH the two subunits are related by crystallographic symmetry.

A comparison of the amino acid sequences shows that there is only a 20–25% sequence identity between the pig cytosolic and mitochondrial MDHs,[4,7] but a 59% sequence identity between *E. coli* MDH and that from pig mitochondria.[9] However, comparisons of the crystal structure have shown a high degree of homology between the three MDH enzymes, particularly at the central core of the proteins. The locations of the substrate and cofactor binding sites are preserved in these three malate dehydrogenases, and the

Color Plates for this article are on page 34.

Address reprint requests to Dr. Duffield at the Division of Biotechnology, PHLS Centre for Applied Microbiology and Research, Public Health Laboratory Service, Porton Down, Salisbury, Wiltshire SP4 0JG, UK.
Received 14 December 1992; revised 26 April 1993; accepted 18 May 1993

catalytically important residues are also conserved. Differences in chain length are generally accommodated in loop regions remote from the subunit interface and the active site.

The stability of the pig cytoplasmic and mitochondrial malate dehydrogenase has been studied. Pig mitochondrial malate dehydrogenase dissociates into monomers and is inactivated at pH 5.0,[10] while cytoplasmic MDH dissociates and is inactivated at pH 2.3.[11] The native oligomeric structure of dimeric malate dehydrogenase is a requirement for efficient catalysis.[10] Therefore, the subunit interface is central to the maintenance of the catalytically competent form of the enzyme.

The pH sensitivity of mMDH is thought to be a result of protonation of HIS 46. HIS 46 is hydrogen bonded to the guanidinium group of ARG 152, but on protonation of the imadazole ring, the two positive charges are located adjacent to each other, resulting in destabilization of the subunit interface and dissociation of the monomers. This effect can be reversed in yeast malate dehydrogenase by mutation of HIS 46 to a leucine, which increases the stability of the dimeric form and causes an acid shift in the pH optimum for catalysis.[12]

Several reports have been made describing the interactions at the subunit interface of pig cytosolic malate dehydrogenase.[4,13] Dissociation of the subunits by heat or chemical denaturants results in a loss of enzyme activity, and it has been postulated that catalytic activity is modulated via the formation of dimers. This is most probably due to the involvement of ARG 161 which participates both in intersubunit interactions as well as in substrate binding.

Denaturation–renaturation studies carried out by Iijima et al.[14] on *Thermus aquaticus* malate dehydrogenase again suggest that enzymatic activity is effected by the formation of dimers, and further suggests that strong subunit interactions play a role in the heat stability of this enzyme. The greater heat stability of glyceraldehyde phosphate dehydrogenase from *Bacillus stearothermophilus* has been shown to be due to three additional salt bridges formed by each subunit to the others in the tetramer.[15]

The gene for *Thermus aquaticus* malate dehydrogenase (tMDH) has been cloned and highly expressed in *E. coli*, making for ease of isolation.[16] The gene has been sequenced[17] and found to differ by 20 bases from the sequence of the gene from *Thermus flavus* MDH,[18] although both translate to an identical amino acid sequence. Comparisons of the MDH amino acid sequences show that there is an identity of 53% between pig cytosolic malate dehydrogenase and *Thermus* malate dehydrogenase, but identities of only 21% and 24% with mMDH and eMDH, respectively.

Thermus aquaticus is a typical gram negative thermophilic bacterium, and many of its enzymes have been purified and characterized. In all cases, the thermal stability of these enzymes has been found to be greater than their mesophilic counterparts,[19–21] the same being true for tMDH which loses no activity after 60 min at 90°C.[22] *Thermus* MDH also shows a greater resistance to chemical denaturants and pH inactivation.[14] Since there are no direct comparisons between pig mMDH and tMDH, the stabilities of the two enzymes toward thermal and chemical denaturation were measured so as to provide a quantitative estimate of their stabilities.

The structure–function relationship of malate dehydrogenase is well characterized and documented,[23] making this enzyme a potentially useful model for examining general hypotheses on thermal stability using the MDH from *T. aquaticus*. As there is a high degree of homology between the known malate dehydrogenase crystal structures, it would seem reasonable to assume that the three-dimensional structure of *Thermus* MDH would also be very similar. cMDH has the greatest sequence identity with tMDH and is therefore considered the best structure on which to base the model of tMDH.

The modeling of a protein onto a homologous crystal structure has been used to predict several structures, the first being α-lactalbumin based on the known structure of hen egg white lysozyme.[24] Comparisons of the three-dimensional structures and subsequent homologous modeling of families of proteolytic enzymes have demonstrated that functionally similar regions of related proteins can be modeled with a high degree of accuracy.[25]

Using the three-dimensional model of *Thermus aquaticus* malate dehydrogenase, the reasons for the increased thermal stability of this enzyme can be more fully examined.

METHODS

Pig malate dehydrogenase was obtained from Sigma Chemical Company, while *Thermus aquaticus* MDH was purified as described previously.[17] Ultrapure guanidinium chloride was obtained from BRL. All other chemicals were of analytical grade or higher. Residue numbering relates to pig cytosolic MDH.

Thermal stability

Irreversible enzyme inactivation was measured in both cases. Enzyme solution was diluted into 20 mM phosphate buffer, adjusted to pH 7.4 at the working temperature, to a final concentration of 0.55 μM subunits. Samples of 50 μl were placed in glass test tubes, which were placed sequentially into holes in a heating block which were filled with silicone oil to ensure good thermal contact. The tubes were incubated over a time course of up to one hour. At the end of the incubation, all of the tubes were removed together and placed on ice for 5 min before the residual enzyme activity was measured. A single tube was kept on ice throughout the experiment as a control. Malate dehydrogenase activity was assayed as described previously.[26]

Guanidinium chloride-induced unfolding

The unfolding of pig and *Thermus* malate dehydrogenases in guanidinium chloride was followed by measuring the change in tryptophan fluorescence emission at 330 nm as a function of denaturant concentration.

Guanidinium chloride was made up as a 5.55-M stock solution in 50 mM potassium phosphate buffer, pH 7.4. The concentration was checked by refractive index measurements.[27] Enzyme, at a concentration of 0.24-μM subunits, was incubated in various concentrations of guanidinium chloride in 50 mM potassium phosphate buffer, pH 7.4, containing 1 mM dithiothreitol, at 22° for 16 h. The degree of unfolding at each concentration of denaturant was determined by measuring the fluorescence emission at 330 nm

after excitation at 295 nm, using a Perkin Elmer LS5 spectrofluorimeter.

The equilibrium constant for the guanidinium chloride-induced unfolding of a protein can be calculated from Equation (1):

$$K_{eq} = (F_N - F)/(F - F_D) \quad (1)$$

where K_{eq} is the equilibrium ratio of denatured-to-native protein, F is the observed fluorescence, and F_N and F_D are the values of the fluorescence for native and denatured protein. The difference in free energy between the native and denatured protein can then be calculated from Equation (2):

$$\Delta G = -RT \ln K_{eq} = -RT \ln [(F_N - F)/(F - F_D)] \quad (2)$$

where R is the gas constant, and T is the absolute temperature. The evaluation of the equilibrium constant at each guanidinium chloride concentration requires the extrapolation of the pre- and post-transition baselines in Figure 2 to be extrapolated into the transition region, using Equation (3):

$$F_N = F_N^\circ + m_N[\text{GdmCl}] \text{ and } F_D = F_D^\circ + m_D[\text{GdmCl}] \quad (3)$$

where F_N° and F_D° are the fluorescence emissions of native and denatured enzyme at zero denaturant concentration, m_N and m_D are the slopes of the pre- and post-transition baselines, and [GdmCl] is the concentration of guanidinium chloride. It has been found experimentally that the free energy of unfolded proteins in the presence of a denaturant is linearly related to the concentration of denaturant:[27,28]

$$\Delta G = \Delta G^\circ - m_G[\text{denaturant}] \quad (4)$$

where ΔG° is the apparent free energy denaturation in the absence of denaturant, and m_G is the dependence of ΔG on denaturant concentration, as shown in Figure 3. Equations (2–4) can be combined into a single expression relating ΔG and the denaturant concentration,[29] giving Equation (5).

$$F = \frac{(F_N + m_N[\text{GdmCl}]) + (F_D + m_D[\text{GdmCl}])\exp\{-(\Delta G^\circ - m_G[\text{GdmCl}]/RT)\}}{1 + \exp\{-(\Delta G^\circ - m_G[\text{GdmCl}]/RT)\}} \quad (5)$$

The observed data were directly fitted to this equation using the nonlinear regression analysis program Enzfitter (Cambridge Biosoft, Cambridge, UK).

Construction of *Thermus* malate dehydrogenase model structure

The three-dimensional coordinates and amino acid sequence of the pig cytosolic malate dehydrogenase were obtained from the Brookhaven Protein Data Bank.[4,30] The *Thermus* and pig MDH amino acid sequences were aligned using the program Bestfit from the Genetics Computer Group (GCG) Sequence Analysis Software Package,[31] and then refined by eye to determine the best location for areas of deletion, allowing for maximal conservation of the polypeptide backbone structure.

Model building was performed on an Evans and Sutherland PS390 graphics system interfaced to a Digital Equipment Corporation Microvax II using the molecular modeling package, SYBYL v5.3 (Tripos Associates, St. Louis, MO).

To construct the model of *Thermus* MDH, the overall structure of the carbon backbone of the pig cytosolic enzyme was maintained except around the two sites of deletion. Where residues were changed, only the side chains were replaced, leaving the backbone unaltered, and retaining the old values of all conformational angles in the new side chains. Substituted residues were subjected to energy minimization. It is realized that small localized differences may occur between the carbon backbone and in the orientation of various side chains between the two enzymes, but it is impossible to predict what these may be. The areas of deletion were also subjected to minimization to relieve any areas of bad contact and steric hindrance. All energy minimizations were carried out using SYBYL's MAXIMIN2 minimization option.

RESULTS

Stability studies

The irreversible thermal inactivation of pig and *Thermus* MDH is shown in Figure 1. The *Thermus* enzyme had a half-life of 34 min at 90°, while the pig enzyme had a half-life of 1.8 min at 60°. At 60° the *Thermus* enzyme showed no detectable loss in activity after 2 h of incubation.

The effect of guanidinium chloride (GdmCl) on the tryptophan fluorescence of pig and *Thermus* MDHs is shown in Figure 2. The values of ΔG° and m_G for both enzymes, determined by nonlinear regression analysis of the data in Figure 2, are shown in Table 1. Because of the initial steep increase in fluorescence that was observed in both enzymes, the early data points were not used in the curve-fitting analysis of the data. For the pig enzyme the points up to 0.2 M, and for *Thermus* the points up to 1.0 M guanidinium

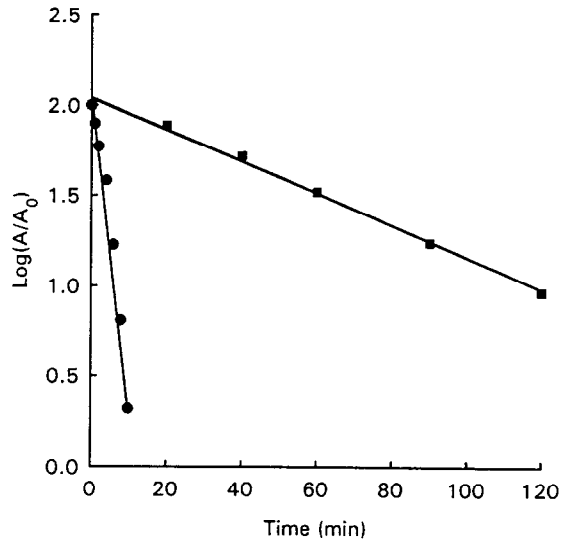

Figure 1. Irreversible thermal inactivation of pig (filled circles) and Thermus *(filled squares) malate dehydrogenases. A is the residual activity after incubation at the specified temperature (90°C for* Thermus *MDH and 60°C for pig MDH), and A_0 is the initial activity.*

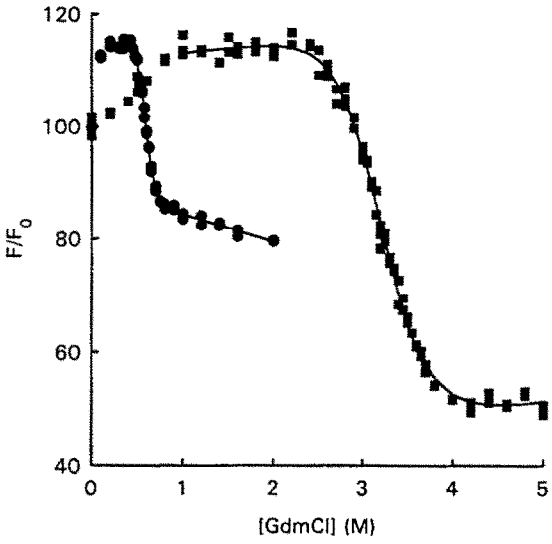

Figure 2. Unfolding of pig (filled circles) and Thermus *(filled squares) malate dehydrogenase in guanidinium chloride. Fluorescence emission is given as the ratio of fluorescence observed under the guanidinium chloride concentrations indicated to that observed in the absence of guanidinium chloride. The solid lines represent the fit of the data using nonlinear regression analysis to Equation (5).*

Table 1. Parameters characterizing the guanidinium chloride-induced unfolding of pig and *Thermus* malate dehydrogenases

	ΔG (kjoule/mol)	m_G (kjoule/mol·M)	$[GdmCl]_{1/2}$ (M)
Pig	−27.0 ± 1.5	−46.0 ± 2.4	0.58
Thermus	−30.9 ± 1.5	−9.6 ± 0.5	3.20

chloride were not used. The effect of guanidinium chloride concentration on the apparent values of ΔG for both enzymes is shown in Figure 3.

Model generation

The amino acid sequence alignment of malate dehydrogenase from pig heart and *Thermus aquaticus*, together with secondary structure information taken from the crystal structure of the pig heart enzyme[30] is shown in Figure 4. In order to conserve the structural and sequence alignments, it was necessary to introduce two areas of deletion into the sequence of the pig enzyme. These deletions are located on the surface of the protein, with the minimum disturbance to the three-dimensional structure, and in particular the catalytic regions. First, a single residue in the pig MDH, SER 276, was removed from an area of random coil. A new peptide bond was created between residues GLU 275 and TYR 277, and these and the neighboring two residues on either side were then subjected to energy minimization.

The other deletion, covering a five-residue region in the pig enzyme, was made between TYR 209 and LYS 213, as shown in Figure 4. This region comprises a single helical turn ($\alpha G'$), preceded by a strand of β-sheet (βJ) and followed by a longer region of α-helix ($\alpha 1G$). After removing the five amino acids which form the single helical turn,

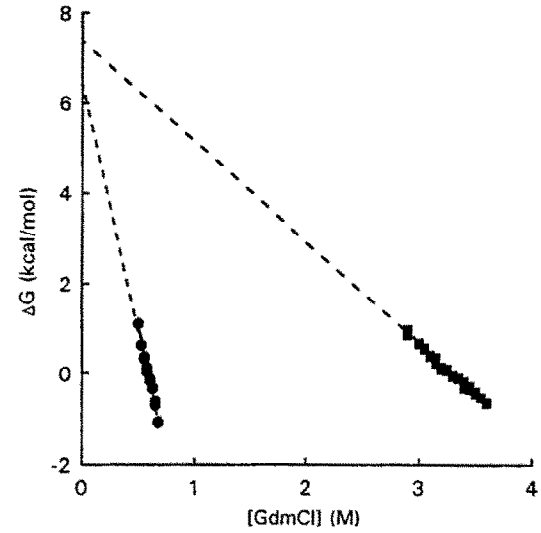

Figure 3. Dependence of ΔG *of pig (filled circles) and* Thermus *(filled squares) malate dehydrogenases on guanidinium chloride concentration. The line is extrapolated to zero denaturant concentration using the values of* $\Delta G°$ *and* m *obtained by the nonlinear regression analysis of the data in Figure 2.*

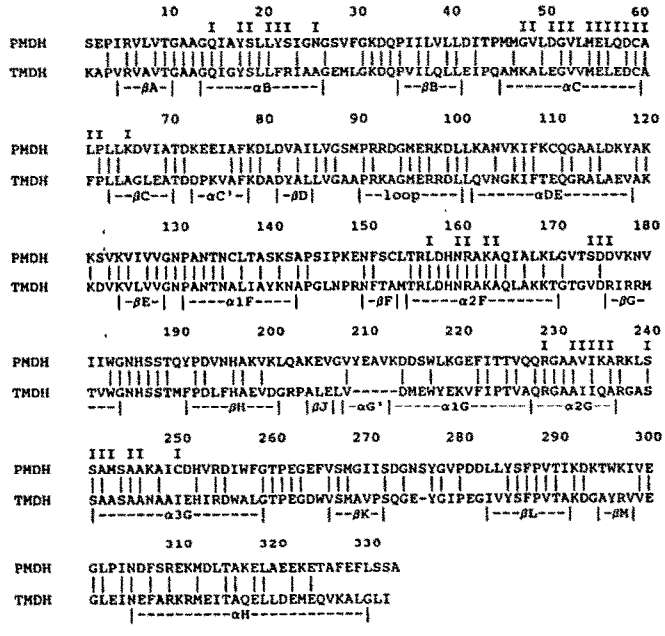

Figure 4. Alignment of the amino acid sequences of malate dehydrogenase from pig heart (PMDH) and Thermus aquaticus *(TMDH). Identical amino acids are indicated by the symbol |. The secondary structure detail is shown beneath the sequence.[41] The symbol I indicates amino acids involved in intersubunit contacts on the Q axis in pig MDH.*

residues VAL 208 and ASP 214 were left 0.73 nm apart. A new peptide bond was formed between these two residues. These two residues and the two neighboring residues on either side of them were subjected to energy minimization. There are however, obvious limitations with this technique. By keeping backbone and main chain conformations unaltered where no substitutions were made, no allowance is made for localized changes in conformation which would occur *in vivo*. From the crystal structure of pig cytosolic MDH it is known that several interactions are made with solvent molecules, but for the sake of simplicity these have been ignored in constructing the *Thermus* MDH model.

Comparison of the two MDH structures

The three major active site residues, ASP 158, ARG 161, and HIS 186 are all completely conserved between the pig cytoplasmic and *T. aquaticus* MDH. These three amino acids are also found at the active site of lactate dehydrogenases, and play a central role in the catalytic process.[6,32] Residues involved in lining the crevice where the substrate and cofactor are located are also conserved between the two MDHs, with either the identical amino acid or a functionally similar one in position, thus preserving the tertiary structures of both the catalytic and the cofactor domains.

Of the other residues that are not conserved between the two MDHs, most (90 out of 148) are found to be on the surface of the molecule rather than in the core. It has been observed in thermostable proteins that lysine and aspartate residues are frequently replaced by arginine and glutamate, respectively,[33,34] and this trend is seen between the pig and *Thermus* MDHs (Table 2) with more surface arginine and glutamate residues in tMDH and fewer lysine and aspartate residues. *Thermus* DNA is extremely G/C rich, and arginine may be preferred over lysine to conserve G/C rich codons in the coding sequence.[17] Overall, however, there are more exposed charged residues in the pig MDH, compared to *Thermus* MDH (136 to 94).

The distribution of hydrophobic residues has also been considered, using the SYBYL supplied list of ALA, GLY, ILE, LEU, MET, PRO, VAL, and TRP as being hydrophobic. Pig MDH was found to have 70 exposed hydrophobic residues, while that of *Thermus* MDH had 86 (Table 3). Overall, the *Thermus* enzyme has more hydrophobic residues (380 to 356), and therefore it also has a greater number of buried hydrophobic residues.

Table 2. Comparison of charged residues between *Thermus* and pig MDH

	Pig		*Thermus*	
	Total	Exposed	Total	Exposed
Arginine	10	5	19	12
Lysine	31	27	18	15
Histidine	4	1	4	1
Aspartate	25	19	17	12
Glutamate	18	14	24	17
Total	88	66	82	57

Table 3. Comparison of exposed hydrophobic residues

Pig	*Thermus*	Pig	*Thermus*
	2A	206V	
3P	3P		207L
30G	30G		215M
36I	36I	220G	
42I	42I		224P
	43P		226V
44P		231A	
45M			236A
46M	46M	258F	258L
47G		261P	261P
	63L	263G	236G
	66G	274G	274G
75I	75V	278G	278G
95M	93A	280P	280P
	95M	288P	288P
100L	100L	301G	301G
113A			302L
	118V	303P	
144P	144P	307F	307F
	145G	314L	314I
147P		327F	307F
171G	171G		328A
172V		329F	329L
	201G	330L	330G
203A	203P		331L
	204A		332I
	205L	333A	

Various amino acid substitutions have been reported as being more favorable to thermal stability.[35,36] X → P or G → X are both said to increase the stability since such substitutions reduce the conformational entropy of a protein in the unfolded state,[37] proline because of its pyrolidine ring structure and removal of glycine because of its lack of a β-carbon atom and its need of more free energy in the folding process to achieve the correct conformation. However, the exact contribution of any substitution will also depend on its precise location. *Thermus* contains 3 more prolines than the pig enzyme, but 5 more glycines.

Subunit interactions

In *Thermus* MDH there are a greater number of hydrophobic interactions between the subunits with 22 hydrophobic residues at the subunit interface, compared with 19 in the pig enzyme. In both MDHs there are three ionic interactions at the subunit interface between amino acid side chains, GLU 55–ARG 237, ASP 58–ARG 229, and ASP 58–ARG 161.[4] However, one hydrogen bond between GLN 57 and ARG 229 at the pig mitochondrial MDH subunit interface is replaced by a hydrogen bond between charged groups in the *Thermus* enzyme, where GLN 57 is substituted by GLU. From the model of *Thermus* MDH, the OE2 atom of GLU 57 lies between 0.27 nm and 0.29 nm away from the NH2 of ARG 229, so that a hydrogen bond can be formed between the two charged groups, rather than an ionic interaction.

Hydrogen bonds between uncharged donors and acceptors can contribute 2.0–7.5 kjoule/mol to the observed association energy, while a hydrogen bond between charged groups can contribute 12.5–25.0 kjoule/mol.[38] A salt bridge is also thought to contribute approximately 12.5 kjoule/mol.[39]

When the subunit interface is displayed as a solvent-accessible surface using the MS program,[40] a cavity is apparent where no contact or interaction seems to occur.[23] In the pig heart enzyme this cavity is bordered by TYR 17, SER 18, TYR 21, and SER 22 from both subunits. In the *Thermus* enzyme the cavity is again bordered by TYR 17 and SER 18, but residues 21 and 22 have become PHE 21 and ARG 22. The positively charged guanidinium group of the arginine residue appears to be buried in the face of the phenyl ring of the phenylalanine residue, allowing for an interaction between the π electron system of PHE with the hydrogen bond donor of the ARG (Color Plates 1 and 2).

DISCUSSION

Enzymes from thermophiles generally show increased stability toward thermal inactivation. This is often associated with increased resistance towards chemical denaturants, as is observed with *Thermus* and pig malate dehydrogenases. However, it must be noted that the thermal inactivation studied is an irreversible process while the guanidine hydrochloride denaturation is a reversible equilibrium process. Given the large differences in thermal stability between the two enzymes, there is a surprisingly small difference of about 4.2 kjoule/mol in the value of ΔG° between the *Thermus* and pig enzymes. In contrast, there is a considerable difference in the value of $[GdmCl]_{1/2}$ for the two enzymes; 0.58 M for the pig enzyme and 3.20 M for the *Thermus* enzyme, as would be expected from the observed stability of the *Thermus* enzyme.

The deletions to the pig MDH sequence made for the construction of the *Thermus* enzyme were made in regions of unstructured protein or were positioned so as to cause the least disruption to the core structure. Their effect on the stability is, however, difficult to predict, but it is possible that the removal of the solvent-exposed loop, caused by the five-residue deletion, may confer some increase in thermal stability. However, since this region is also absent from all known sequences of mesophilic mitochondrial MDHs, which do not show any marked differences in stability to the cytosolic forms of the enzyme, it cannot be solely responsible for the increase in thermal stability.

It has been reported that incorrectly folded structures have significantly larger solvent-accessible surfaces.[41] Out of the 90 substitutions made at the molecular surface of *Thermus* MDH, an overall increase of 16 hydrophobic residues is seen. However, although the large number of substitutions at the molecular surface may increase the number of solvent-exposed residues, it also keeps to a minimum the number of changes made to the core structure and functionality of the protein. Experimental work has also shown that substitutions to solvent-exposed residues have little or no effect on the thermal stability of an enzyme. However, an increase in buried hydrophobic residues could be involved in increasing thermal stability.[42]

The increase in the number of prolines in the *Thermus* enzyme could be contributing to its greater stability. The pyrolidine ring of proline restricts the conformations it can adopt, and therefore less free energy is required during folding to achieve the correct conformation. However, substitutions to prolines can also be detrimental, such as in a helix where it would result in destabilization of the helix. Such a substitution is seen in *Thermus* MDH where THR 224 becomes PRO. On consideration of the other substitutions made in helix $\alpha 1G$, and using the parameters by Chou and Fasman, the overall effect is, however, one of stabilization of this helix. Since this particular helix is found directly after the five-residue deletion from pMDH to tMDH, and it could it also be argued that this proline is necessary to relax strain caused by the deletion.

T. aquaticus MDH has a greater number of subunit–subunit interactions which may be partially responsible for the increase in thermal stability, as was previously predicted.[14] A hydrogen bond between uncharged groups replaced by one between charged groups across the *Thermus* subunit interface, coupled with an increase in hydrophobic residues at the subunit interface.

In addition, there is an apparent interaction between the phenylalanine and arginine residues around the cavity. Interactions between charged amino groups and aromatic rings have been observed.[43,44]

Burley and Petsko[43] found that the amino groups of some buried lysine, arginine, asparagine, and glutamine residues were located between 0.34 nm and 0.6 nm of the centroid of the aromatic ring of phenylalanine, tyrosine and tryptophan more frequently than random close packing of side chains would suggest. The $\delta(+)$ of the amino group makes van der Waals contact with the $\delta(-)$ π electrons of the aromatic ring and avoids the $\delta(+)$ of the ring edge. In the *Thermus* MDH dimer, PHE 21 and ARG 22 from different monomers are separated by about 0.35 nm. Quantum mechanical energy calculations suggest that interactions between amino groups and aromatic rings are enthalpically favorable, and that such interactions contribute between 4 kjoule/mol and 10 kjoule/mol of stabilizing enthalpy.[43,45] It has been suggested that such interactions may make an important contribution to the stability of proteins. The close proximity of an aromatic side chain to a charged histidine ring has been found to contribute about 4 kjoule/mol of stabilizing energy in barnase.[44] Such favorable interactions have been suggested to have a more important role in stabilizing protein structures than otherwise thought, and may account in part, therefore, for the greater stability of *Thermus* MDH.

The stability of malate dehydrogenase from mitochondria, cytoplasm, and *Thermus* has been studied, and the strength of the intersubunit interaction shown to increase in the order mitochondrial < cytoplasmic < *Thermus*. Our model of *Thermus* MDH supports the view that the increased stability is due to the increased number of interactions across the subunit interface. However, although the *Thermus* MDH model is very useful for providing information about the subunit–subunit interactions and the thermal stability of this enzyme, a full understanding of such interaction can only be obtained when a full crystal structure is known. A preliminary X-ray diffraction analysis of a mutant of *T. flavus* MDH has already been reported,[46] but no coordinates are yet available in the Brookhaven Protein Data Bank. It is most likely that the increased thermal stability of

Thermus malate dehydrogenase results as the additive effect of several independent substitutions.

ACKNOWLEDGEMENTS

The authors are grateful to the Department of Trade and Industry for their support.

REFERENCES

1 Chien, S.M. and Freeman, K.B. Import of rat liver mitochondrial malate dehydrogenase. *J. Biol. Chem.* 1984, **259,** 3337–3343

2 Hill, E., Tsernoglou, D., Webb, L., and Banaszak, L.J. Polypeptide conformation of cytoplasmic malate dehydrogenase from an electron density map at 3-Å resolution. *J. Mol. Biol.* 1972, **72,** 577–591

3 Webb, L.E., Hill, E.J., and Banaszak, L.J. Conformation of nicotinamide adenine dinucleotide bound to cytoplasmic malate dehydrogenase. *Biochemistry.* 1973, **12,** 5101–5108

4 Birktoft, J.J., Rhodes, G., and Banaszak, L.J. Refined crystal structure of cytoplasmic malate dehydrogenase at 2.5-Å resolution. *Biochemistry.* 1989, **28,** 6065–6981

5 Weininger, M., Birktoft, J.J., and Banaszak, L.T. In: *Pyridine nucleotide dependent dehydrogenases* (H. Sund, Ed.), Walter de Gruyter, Berlin, 1977, pp. 87–98

6 Birktoft, J.J. and Banaszak, L.J. The presence of a histidine-aspartic acid pair in the active site of 2-hydroxyacid dehydrogenase. *J. Biol. Chem.* 1983, **258,** 472–482

7 Roderick, S.L. and Banaszak, L.J. The three-dimensional structure of porcine heart mitochondrial malate dehydrogenase at 3.0-Å resolution. *J. Biol. Chem.* 1986, **261,** 9461–9464

8 Hall, M.D., Levitt, D.G., and Banaszak, L.J. Crystal structure of *Escherichia coli* malate dehydrogenase. A complex of the apoenzyme and citrate at 1.87-Å resolution. *J. Mol. Biol.* 1992, **226,** 867–882

9 McAlister-Henn, L., Blaber, M., Bradshaw, R.A., and Nisco, S.J. Complete nucleotide sequence of the *Escherichia coli* gene encoding malate dehydrogenase. *Nucleic Acid Res.* 1987, **15,** 4993

10 Bleile, D.M., Schulz, R.A., and Harrison, J.H. Investigation of the subunit interactions in malate dehydrogenase. *J. Biol. Chem.* 1977, **252,** 755–758

11 Rudolph, R., Fuchs, I., and Jaenicke, R. Reassociation of dimeric cytoplasmic malate dehydrogenase is determined by slow and very slow folding reactions. *Biochemistry.* 1986, **25,** 1662–1669

12 Steffan, J.S. and McAlister-Henn, L. Structural and functional effects of mutations altering the subunit interfaces of mitochondrial malate dehydrogenase. *Arch. Biochem. Biophys.* 1991, **287,** 276–282

13 Birktoft, J.J., Fu, Z., Carnahan, G.E., Rhodes, G., Roderick, S.L., and Banaszak, L.J. Comparison of the molecular structures of cytoplasmic and mitochondrial malate dehydrogenases. *Biochem. Soc. Trans.* 1989, **17,** 301–304

14 Iijima, S., Saiki, T., and Beppu, T. Reversible denaturation of thermophilic malate dehydrogenase by guanidinium chloride and acid. *J. Biochem. (Tokyo).* 1984, **95,** 1273–1281

15 Biesecker, G., Harris, J.I., Thierry, J.-C., Walker, J.E., and Wonacott, A.J. Sequence and structure of D-glyceraldehyde-3-phosphate dehydrogenase from *Bacillus stearothermophilus*. *Nature (London).* 1977, **266,** 328–333

16 Alldread, R.M., Nicholls, D.J., Sundaram, T.K., Scawen, M.D., and Atkinson, T. Over-expression of the *Thermus aquaticus* B malate dehydrogenase gene in *E. coli*. *Gene.* 1992, **114,** 139–143

17 Nicholls, D.J., Sundaram, T.K., Atkinson, T., and Minton, N.P. Cloning and nucleotide sequences of the *mdh* and *sucD* genes from *Thermus aquaticus* B. *FEMS Microbiol. Lett.* 1990, **70,** 7–14

18 Nishiyama, M., Matsubara, N., Yamamoto, K., Iijima, S., Uozumi, T., and Beppu, T. Nucleotide sequence of the malate dehydrogenase gene of *Thermus flavus* and its mutation directing an increase in enzyme activity. *J. Biol. Chem.* 1986, **261,** 14178–14183

19 Curran, M.P., Daniel, R.M., Guy, G.R., and Morgan, H.W. A specific L-asparaginase from *Thermus aquaticus*. *Arch. Biochem. Biophys.* 1985, **241,** 571–576

20 Eguchi, H., Wakagi, T., and Oshima, T. A highly stable NADP-dependent isocitrate dehydrogenase from *Thermus thermophilus* HB8: purification and general properties. *Biochim. Biophys. Acta.* 1989, **990,** 133–137

21 Hocking, J.D. and Harris, J.I. D-glyceraldehyde-3-phosphate dehydrogenase: Amino-acid sequence of the enzyme from the extreme thermophile *Thermus aquaticus*. *Eur. J. Biochem.* 1980, **108,** 567–579

22 Iijima, S., Saiki, T., and Beppu, T. Physicochemical and catalytic properties of thermostable malate dehydrogenase from an extreme thermophile *Thermus flavus* AT-62. *Biochim. Biophys. Acta.* 1980, **613,** 1–9

23 Banaszak, L.J. and Bradshaw, R.A. In: *The Enzymes.* (P. Boyer, Ed.), Academic Press, New York, 1975, pp. 369–396

24 Browne, W.J., North, A.C.T., and Phillip, D.C. A possible three-dimensional structure of bovine α-lactalbumin based on that of hen's egg-white lysozyme. *J. Mol. Biol.* 1969, **42,** 65–67

25 Siezen, R.S., de Vos, W.M., Leunissen, J.A.M., and Dijkstra, B.W. Homology modeling and protein engineering strategy of subtilases, the family of subtilisin-like serine proteases. *Protein. Eng.* 1991, **4,** 719–737

26 Smith K., Sundaram, T.K., Kernick, M., and Wilkinson, A.E. Purification of bacterial malate dehydrogenase by selective elution from a triazinyl dye affinity column. *Biochim. Biophys. Acta.* 1982, **708,** 17–25

27 Pace, C.N. Determination and analysis of urea and guanidine hydrochloride denaturation curves. *Methods Enzymol.* 1986, **131,** 266–280

28 Pace, C.N., Shirley, B.A., and Thompson, J.A. In: *Protein structure* (T.E. Creighton, Ed.), IRL Press, Oxford, 1989, pp. 311–330

29 Santoro, M.M. and Bolen, D.W. Unfolding free energy changes determined by the linear extrapolation method. 1. Unfolding of phenylmethanesulphonyl α-chymotryp-

sin using different denaturants. *Biochemistry*. 1988, **27**, 8063–8068
30 Birktoft, J.J., Bradshaw, R.A., and Banaszak, L.J. Structure of porcine heart cytoplasmic malate dehydrogenase: Combining X-ray diffraction and chemical sequence data in structural studies. *Biochemistry*. 1987, **26**, 2722–2734
31 Devereux, J., Haeberli, P., and Smithies, O. A comprehensive set of sequence analysis programs for the VAX. *Nucleic Acid Res*. 1984, **12**, 387–395
32 Clarke, A.R., Wilks, H.M., Barstow, D.A., Atkinson, T., Chia, W.N., and Holbrook, J.J. An investigation of the contribution made by the carboxylate group of an active site histidine-aspartate couple to binding and catalysis in lactate dehydrogenase. *Biochemistry*. 1988, **27**, 1617–1622
33 Qaw, F.S. and Brewer, J.M. Arginyl residues and thermal stability in proteins. *Molec. Cell. Biiochem*. 1986, **71**, 121–127
34 Mrabet, N.T., Van den Broeck, A., Van den Brande, I., Stanssens, P., Laroche, Y., Lambeir, A.-M., Matthijssen, G., Jenkins, J., Chiadmi, M., van Tilbeurgh, H., Rey, F., Janin, J., Quax, W.J., Lasters, I., De Maeyer, M., and Wodak, S.J. Arginine residues as stabilizing elements in proteins. *Biochemistry*. 1992, **31**, 2239–2253
35 Argos, P., Rossmann, M.G., Grau, U.M., Zuber, H., Frank, G., and Tratschin, J.D. Thermal stability and protein structure. *Biochemistry*. 1979, **18**, 5698–5703
36 Matsumura, M., Becktel, W.J., and Matthews, B.W. Hydrophobic stabilization in T4 lysozyme determined directly by multiple substitutions of Ile 3. *Nature (London)*. 1988, **334**, 406–410
37 Matthews, B.W., Nicholson, H., and Becktel, W.J. Enhanced protein thermal stability from site-directed mutations that decrease the entropy of unfolding. *Proc. Natl. Acad. Sci. USA*. 1987, **84**, 6663–6667
38 Fersht, A.R. The hydrogen bond in molecular recognition. *Trend. Biochem. Sci*. 1987, **12**, 301–304
39 Fersht, A.R. Conformational equilibria in α- and δ-chemotrypsin. The energetics and importance of the salt bridge. *J. Mol. Biol*. 1972, **64**, 497–509
40 Connolly, M.L. Solvent-accessible surface of proteins and nucleic acids. *Science*. 1983, **221**, 709–713
41 Novotny, J., Bruccoleri, R., and Karplus, M. An analysis of incorrectly folded protein models. *J. Mol. Biol*. 1984, **177**, 787–818
42 Hecht, M.H., Sturtevant, J.M., and Sauer, R.T. Effect of single amino acid replacements on the thermal stability of the NH_2-terminal domain of phage lambda repressor. *Proc. Natl. Acad. Sci. USA*. 1984, **81**, 5685–5689
43 Burley, S.K. and Petsko, G.A. Amino–aromatic interactions in proteins. *Febs. Lett*. 1986, **203**, 139–143
44 Loewenthal, R., Sancho, J., and Fersht, A.R. Histidine–aromatic interactions in barnase. *J. Mol. Biol*. 1992, **224**, 759–770
45 Levitt, M. and Perutz, M.F. Aromatic rings act as hydrogen bond acceptors. *J. Mol. Biol*. 1988, **201**, 751–754
46 Kelly, C.A., Sarfaty, S., Nishiyama, M., Beppu, T., and Birktoft, J.J. Preliminary X-ray diffraction analysis of a crystallizable mutant of malate dehydrogenase from the thermophile *Thermus flavus*. *J. Mol. Biol*. 1991, **221**, 383–385